

Oct 2013

Aquatic Ecodynamics (AED) Model Library

Science Manual

DRAFT v4 (Oct 2013)

M.R. Hipsey, L.C. Bruce & D.P. Hamilton



THE UNIVERSITY OF
WESTERN AUSTRALIA
Achieve International Excellence



Summary

This report outlines the Aquatic Ecodynamics (AED) modelling library - an open-source community-driven library of model components for simulation of “aquatic ecodynamics”. The model has been developed researchers at UWA to plug into the FABM framework, or alternatively the library components can also be called directly from other software applications. The model can therefore be used in a wide range of spatial contexts – including with 0D, 1D, 2D and 3D models that are able to simulate the aquatic environment.

In particular the AED library consists of numerous modules that are designed as individual model ‘components’ able to be configured in a way that facilitates custom aquatic ecosystem conceptualisations – either simple or complex. These may be relevant to specific water quality problems or aquatic ecosystem investigations. Users select water quality and ecosystem variables they wish to simulate and then are able to customize connections and dependencies with other modules, thereby constructing relevant interactions and feedbacks that may be occurring within an aquatic system. The code also allows for easy customisation at an algorithm level how model components operate (e.g. photosynthesis functions, sorption algorithms etc.). In general, model components consider the cycling of carbon, nitrogen and phosphorus, and other relevant components such as oxygen, and are able to simulate organisms including different functional groups of phytoplankton and zooplankton, and also organic matter. Modules to support simulation of water column and sediment geochemistry, including coupled kinetic-equilibria interactions, are also included.

This document summarises the mathematical basis for the balance equations and interactions between the modules. In addition a summary of parameter values for lake, river and estuary environments are also summarized from a range of sources.

Contents

SUMMARY	2
CONTENTS	3
<u>AQUATIC ECODYNAMICS (AED) MODEL APPROACH</u>	4
OVERVIEW	4
THE FRAMEWORK FOR AQUATIC BIOGEOCHEMICAL MODELS (FABM)	4
Available hydrodynamic driver platforms	6
Other candidate biogeochemical models	7
Further information on FABM	7
<u>AED MODULE DESCRIPTIONS</u>	8
OVERVIEW	8
MODULE CONCEPTUALIZATION	8
MODULE DESCRIPTIONS	10
General Notation	10
Light	10
Dissolved Oxygen	11
Carbon, Nitrogen, Phosphorus and Silica: aed_carbon, aed_nitrogen, aed_phosphorus, aed_silica, aed_organic_matter	12
Phytoplankton Dynamics – aed_phytoplankton	19
Zooplankton Dynamics – aed_zooplankton	24
Suspended Sediment & Turbidity : aed_tracer, aed_totals	25
Geochemical Dynamics : aed_geochemistry, aed_iron, aed_sulfur	25
Sediment Biogeochemistry – aed_sedflux, aed_seddiagenesis	25
Pathogens – aed_pathogens	25
PARAMETER SUMMARY	25
<u>CONFIGURING THE AED LIBRARY</u>	30
<u>REFERENCES</u>	32

Aquatic Ecodynamics (AED) Model Approach

Overview

This document outlines the **Aquatic Ecodynamics (AED) modelling library** - an open-source community-driven library of model components for simulation of “*aquatic ecodynamics*”, referring to water quality and general aquatic ecosystem dynamics. The model library has been primarily designed as a plugin to the FABM framework, described below, or alternatively the library objects and functions can also be called directly from other software applications.

Modern analyses of aquatic environments requires flexibility to join a range of coupled models of hydrodynamics/hydrology, biogeochemistry and aquatic ecology, however many model frameworks make this difficult due to rigid model structures. A major barrier identified is the simple practical aspect that there are lots of models and model approaches, but limited open-source codes and standards that bind the community or facilitate integration (Mooij et al., 2010; Trolle et al., 2012), and there has been limited comparisons of the most suitable types of models structures for different applications. There has also been *difficulty in linking between biogeochemical models of diverse aquatic systems* in real world complex landscapes. There is therefore a need for model systems that can cover a range of spatial dimensionality and system integration and frameworks that can use a diverse array of physical drivers (e.g., wetland/floodplain model, river model, lake model, estuary model) to couple with biogeochemical and/or ecological ‘components’ (e.g., see Figure 1).

The general philosophy of the AED library has been to create a software tool-kit that is easily customisable, fast to develop, accessible to non-developers, and contains a large range of options for different process parameterisations. In doing so, the aims is to create a widely-used code-base that evolves to include a diverse range of approaches to the simulation of a diverse range of aquatic applications. Through the FABM framework or custom model interfaces the library can be used to innovate a variety of model conceptualisations and link to numerous physical models.

In particular it has been used for numerous inland water applications, both lotic and lentic systems with numerous applications to lake, river and estuarine systems.

The Framework for Aquatic Biogeochemical Models (FABM)

The *Framework for Aquatic Biogeochemical Models* (FABM) is a relatively new code-base designed to facilitate the simulation of aquatic biogeochemical and ecological dynamics. It has been developed as an alternative to existing rigid water quality modelling approaches as much present-day software does not address the challenges faced in model coupling and a recognized need to develop improved standards and flexibility in model integration in concert with an active development community (Trolle et al., 2012). The basic framework has been developed by Dr. Jorn Bruggeman and colleagues under the EU7 project “Marine Ecosystem Evolution in a Changing Environment” (MEECE), and readers are referred to Bruggeman (2011) for further background.

FABM itself is not a water quality model, but rather it is a code framework (“API”) that facilitates integration of different biogeochemical/ecological model approaches and to enable coupling of these with a diverse array of physical (hydrodynamic) driver models. Therefore, its intention is not to be a

sophisticated “model of everything”, but users can configure it to be as simple or as complicated as desired. It supports numerous biogeochemical and ecological models from various developers with different approaches and varied applications.

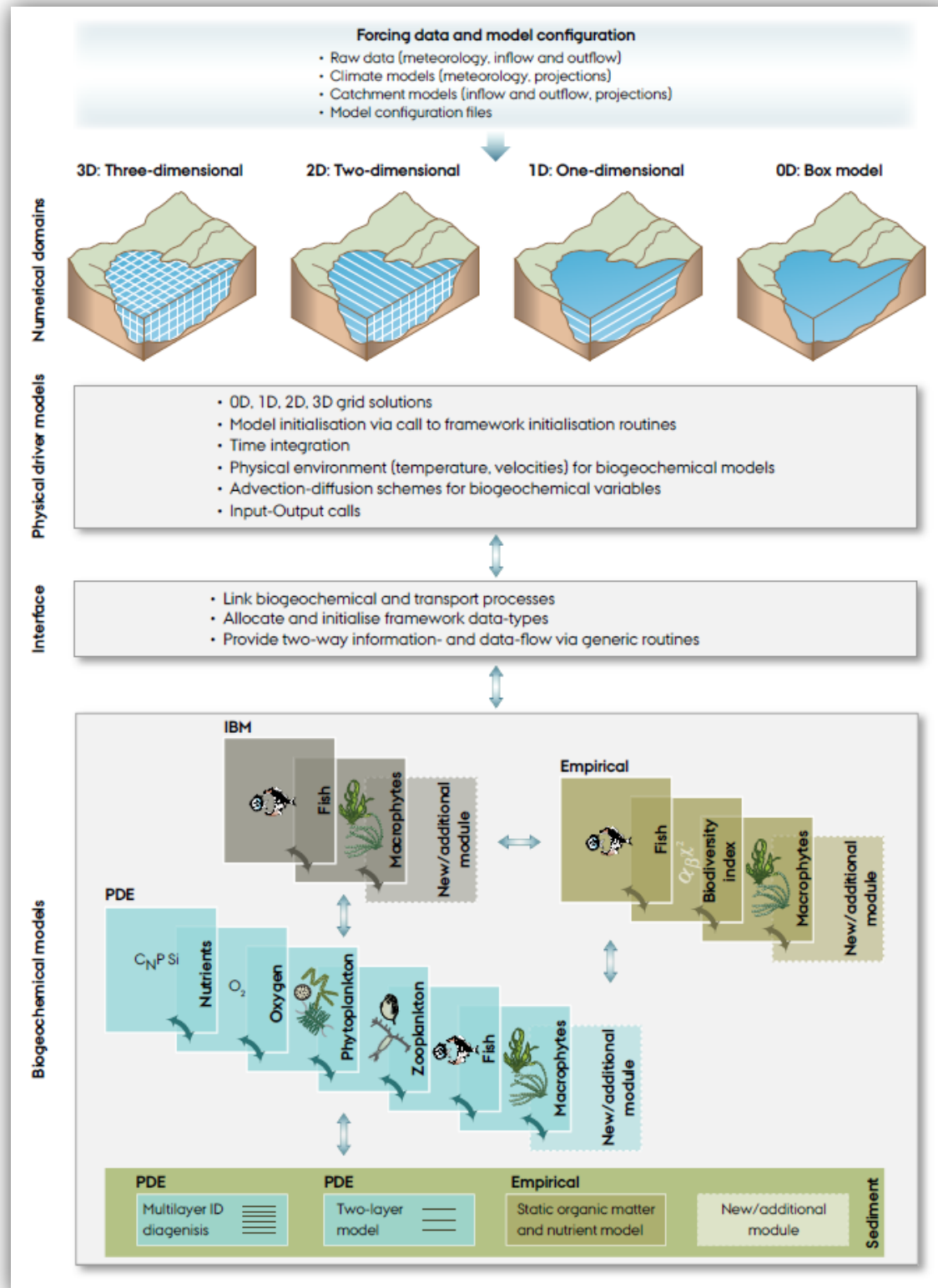


Figure 1: Schematic representation of coupling and biogeochemical modelling approach
(taken from Trolle et al., 2012).

Available hydrodynamic driver platforms

The underlying framework allows a flexible coupling interface to hydrodynamic models, and at its core it consists of a thin layer of code designed to manage communication and data exchange, through programming interfaces which a physical host (hydrodynamic model) and any number biogeochemical models pass information. It has been applied across numerous types of aquatic systems ranging from the global ocean via its coupling to MOM4 and GOTM, to estuaries and coasts via its coupling to the model GETM, and to lakes and reservoirs via its coupling to the 1D lake model GLM.

The model adopts a standard interface so that the code itself can be coupled with other forms of hydrodynamic models, or it can be run in isolation (0D) for hypothesis testing and ecological model prototyping. The advantage of the FABM approach over other platforms is its flexibility for coupling a diverse array of model approaches and its support for rigorous numerical solution schemes (e.g., Burchard *et al.*, 2005; Broekhuizen *et al.*, 2008) that are known to be important in achieving accurate solutions of complex biogeochemical model equation sets. Its code structure is also designed to be work well when used with parallel processors.

Users who can couple their hydrodynamic model with FABM - see instructions here: http://sourceforge.net/apps/mediawiki/fabm/index.php?title=Coupling_FABM_to_a_new_physical_model - can access the AED library in addition to numerous other models currently implemented as outlined next.

Table 1: Current physical driver models linked to FABM (also refer to <http://sourceforge.net/apps/mediawiki/fabm/index.php>).

Name	Dimensionality	Stratification	Comments
0D Driver	0D	-	Simple 'box' model for testing biogeochemical model operation
General Ocean Turbulence Model (GOTM)	1D	Library of range of simple and complex mixing approaches	Widely used library of vertical mixing algorithms http://www.gotm.net
General Estuarine Transport Model (GETM)	3D structured grid, with curvilinear option	Uses GOTM turbulence library	Open-source coastal/estuarine model http://www.getm.eu
Modular Ocean Model version 4 (MOM4)	3D		Widely used global ocean model http://www.gfdl.noaa.gov/fms
General Lake Model (GLM)	1D (vertical) – Lagrangian layered grid	Custom vertical mixing algorithms	Includes Ice cover Simple to use http://aed.see.uwa.edu.au/research/models/GLM/
TUFLOW-FV	3D (finite volume)	Several approaches available	Coupled model has been applied (Bruce <i>et al.</i> , 2013), but currently not available for general use.

Other candidate biogeochemical models

The AED modules described here that link to FABM are in addition to other common biogeochemical configurations such as the ‘Fasham’ model template (currently the most highly cited aquatic biogeochemical model approach; Arhonditsis *et al.* 2006), ERSEM, and ERGOM, as well as simple ‘NPZD’ model templates (e.g. Burchard *et al.* 2006). The range of ecosystem models that are implemented within the FABM framework are summarised briefly in Table 2, and since the focus of this document is the AED models, readers are referred to FABM documentation and associated references for details of the other models.

Table 2: Current coupled aquatic biogeochemical models included within the FABM framework.

Name	Description
pml/ carbonate	Carbonate chemistry
pml/ ersem	European Regional Seas Ecosystem Model
metu/ mnemiopsis	population model for Mnemiopsis
gotm/ npzd	Simple NPZD model (Burchard <i>et al.</i> , 2005), ported from GOTM
gotm/ fasham	Fasham <i>et al.</i> (1990) model with modifications by, ported from GOTM
iow/ ergom	Baltic Sea Research Institute ecosystem model
examples/ benthic	Example of a benthic predator
aed/ ...	<i>Aquatic Ecodynamics Library</i> <i>(focus of this report, described in the next section)</i>
	Oxygen Nitrogen Phosphorus Silica Organic Matter Phytoplankton Zooplankton Sediment Diagenesis Geochemistry Pathogens

Further information on FABM

For more information on the code structure and approach of FABM the reader is referred to Bruggerman *et al.* (2011).

FABM documentation, code and test cases are currently available from a Git repository at SourceForge: <http://sourceforge.net/apps/mediawiki/fabm/index.php>.

The contents of this repository can be obtained on UNIX/Linux/Mac OS X systems by executing:

```
git clone git://fabm.git.sourceforge.net/gitroot/fabm/fabm
```

AED Module Descriptions

Overview

The philosophy of the AED modules is that individual model ‘components’ can be configured in a way that facilitates custom aquatic ecosystem configurations. Users select modules they are wishing to simulate and then are able to customize connections with other modules. The modules exist within a hierarchy of dependencies, and connections must be set in the right order.

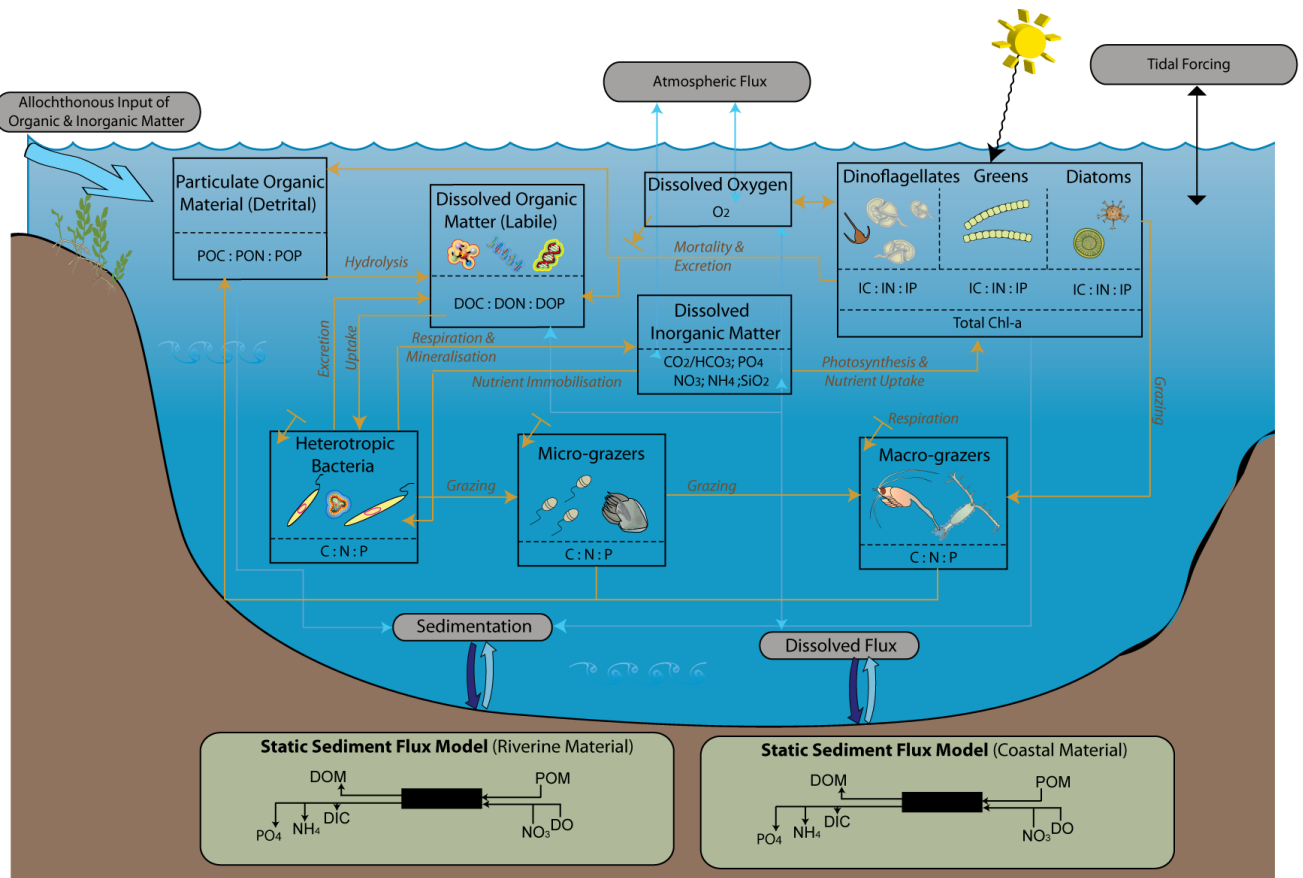
In general, model components consider the cycling of carbon, nitrogen and phosphorus, and other relevant components such as oxygen, and are able to simulate organisms including different functional groups of phytoplankton and zooplankton, and also organic matter. Much of the science basis and mathematical approach implemented in the AED modules is similar to similar models that have been used over the past two decades, and include many similarities to widely used approaches such as CAEDYM, CE-QUAL-W2, WASP and numerous others. The modules, however, are implemented within the FABM numerical framework and include numerous different process representations over these earlier studies, and are reported in detail below.

Module conceptualization

Whilst the AED modules are highly flexible and can be customised for user-defined biogeochemical and ecological configurations, they have generally been designed to simulate the interactions between nutrients, organic matter, phytoplankton and zooplankton. When coupled with the hydrodynamic driver, the modules allow for a comprehensive simulation of processes that govern the transport and fate of water quality attributes included suspended sediment, dissolved inorganic nutrients, organic matter (dissolved and particulate), phytoplankton and zooplankton, and relevant fluxes at the air-water and sediment-water interface. Given the flexible nature of model integration, multiple identical modules can be simulated allowing the user to further partition ecological components, for example, two organic matter modules can be enabled with unique parameters for each to reflect labile versus refractory material in a simulation. Similarly, multiple phytoplankton sub-modules can be configured allow for groups of functional types or groups of similar species to be configured. Other modules describing pathogens, and aqueous geochemistry may also be configured.

The modules together simulate the C, N, P, DO, and Si cycles including inorganic nutrient, organic matter, phytoplankton, and zooplankton. In a typical application (Figure 2) several phytoplankton groups (e.g., bacillariophytes / diatoms, D; chlorophytes or green algae, G; cyanobacteria or blue-green algae, B; etc.) would be simulated with zero or more zooplankton groups. Such a configuration would require around nine state variables are required to model the algal biomass (A_D , A_G , A_B) if the dynamically calculated internal nutrient stores of N (PHY_N_D , PHY_N_G , PHY_N_B) and P (PHY_P_D , PHY_P_G , PHY_P_B), and five dissolved inorganic nutrients (FRP, NO₃, NH₄, PIP, RSi), three dissolved (DOC, DON, DOP) and three particulate (POC, PON, POP) detrital organic matter groups, and dissolved oxygen (DO). With a two zooplankton groups configured this constitutes around 24 state variables, all of which are transported and subject to boundary forcing by the hydrodynamic driver.

A general summary of the key modules is included below and detailed equations and parameter descriptions and typical values used are presented in the following section.



Carbon & Nutrient Flux Pathways



Figure 2: AED module conceptual model of carbon and nutrient flux pathways and planktonic groups.

Module descriptions

In this section the detailed model mass balance and biogeochemical algorithms are described. These are not organized by AED modules, but rather based on the element or ecosystem component in line with the conceptual model.

Note that all balance equations in effect also have terms for advection, dispersion, turbulent mixing, and inflows and outflow boundary conditions, however these are highly specific to the particular hydrodynamic driver being used to run the AED or FABM-AED models. Due to potential differences between them, they are not included in the below expressions and the equations presented here solely focus on biogeochemical and ecological interactions. From a numerical perspective this is also consistent since AED processes are split from the numerical solution of the transport-reaction equations and solved sequentially after transport has taken place.

General Notation

N	= number of groups [integer]
a, om, z	= indices of various sub-groups of phytoplankton, organic matter and zooplankton [integer]
$\chi_{C:Y}^{group}$	= the stoichiometric ratio of “group” between C and element “ Y ” [mmol C/mmol Y]
$f_{process}^{var}$	= function that returns the mass flux of “ $process$ ” on “ var ” [mmol var/time]
$R_{process}^{var}$	= the rate of “ $process$ ” influencing the variable “ var ” [/time]
F_{max}^{var}	= the maximum benthic areal flux of variable “ var ” [mmol var/area/time]
p_{source}^{group}	= the preference of “ $group$ ” for “ $source$ ” [0-1]
$\Phi_{lim}^{group}(var)$	= dimensionless limitation or scaling function account for the effect of “ lim ” on “ $group$ ” [-]
k^{var}	= used to identify a generic fraction related to “ var ” [0-1]
Θ_{config}^{group}	= switch to configure selectable model component “ $config$ ” for a specific “ $group$ ” [0,1,2,...]
$c, \theta, \gamma \dots$	= coefficient [various units]

Light

Incident shortwave radiation is supplied by the hydrodynamic driver, where it is used for surface thermodynamics calculations, to FABM. For primary production, the shortwave (280-2800 nm) intensity at the surface is usually converted to the photosynthetically active component (PAR) based on the assumption that ~45% of the incident spectrum lies between 400-700 nm (eg. Jellison and Melack, 1993; Kirk, 1994). PAR penetrates into the water column according to the Beer-Lambert Law. The light extinction coefficient is able to be dynamically adjusted to account for variability in the concentrations of algal, inorganic and detrital particulates, and dissolved organic carbon levels based on user defined specific attenuation coefficients.

$$K_d = K_w + K_e SS + K_e DOC + K_e POC + \sum_a^{N_{PHY}} K_{e_a} PHY c_a$$

Dissolved Oxygen : aed_oxygen

DO dynamics account for atmospheric exchange, sediment oxygen demand, microbial use during organic matter mineralisation and nitrification, photosynthetic oxygen production and respiratory oxygen consumption, and respiration by other optional biotic components. Atmospheric exchange is based on the model of Wanninkhof (1992) and the flux equation of Riley and Skirrow (1974). A simple sediment oxygen demand flux is currently implemented that varies as a function of the overlying water temperature and dissolved oxygen levels. Microbial activity facilitates the breakdown of organic carbon (in particular, DOC) to CO₂, and a stoichiometrically equivalent amount of oxygen is removed. The process of nitrification also requires oxygen that is dependent on the stoichiometric factor for the ratio of oxygen to nitrogen and the half-saturation constant for the effect of oxygen limitation. Photosynthetic oxygen production and respiratory oxygen consumption is summed over the number of simulated phytoplankton groups.

Table 3: Mass balance and functions related to oxygen cycling.

<p><u>State variable mass balance equation:</u></p> $\frac{dO_2}{dt} = \pm f_{atm}^{O_2} - f_{sed}^{O_2} - \frac{f_{miner}^{DOC}}{\chi_{C:O_2}^{miner}} - \frac{f_{nitrif}}{\chi_{N:O_2}^{nitrif}} + \sum_a^{N_{PHY}} \left(\frac{f_{uptake}^{PHY-Ca}}{\chi_{C:O_2}^{PHY}} \right) - \sum_a^{N_{PHY}} \left(\frac{f_{resp}^{PHY-Ca}}{\chi_{C:O_2}^{PHY}} \right) - \sum_z^{N_{ZOO}} \left(\frac{f_{resp}^{ZOO_z}}{\chi_{C:O_2}^{ZOO}} \right)$ <ul style="list-style-type: none"> = ± atmospheric O₂ exchange ± sediment O₂ demand <ul style="list-style-type: none"> - O₂ consumption by mineralisation of DOC (bacterial respiration) - O₂ consumption by nitrification + O₂ production by photosynthesis - O₂ consumption by phytoplankton respiration - O₂ consumption by zooplankton respiration 	
<p><u>Process parameterisations:</u></p> $f_{atm}^{O_2} = \begin{cases} \frac{c_{atm}^{O_2}([O_2]_{atm} - [O_2]_z)}{dz_s} & \text{if } z = z_s \\ 0 & \text{if } z \neq z_s \end{cases}$ <p style="text-align: right;">atmospheric oxygen exchange</p> $f_{sed}^{O_2} = F_{max}^{O_2} \frac{O_2}{K_{sed}^{O_2} + O_2} (\theta_{sed}^{O_2})^{T-20} \left(\frac{\widehat{A}_z}{dz_z} \right)$ <p style="text-align: right;">sediment oxygen demand (SOD)</p> <p>where $\widehat{A}_z = A_z^{ben}/A_z$ and dz_z is the thickness of the z^{th} layer/cell.</p>	
<p><u>Diagnostic & derived outputs:</u></p> <p>Oxygen saturation</p> <p><i>OXYPC</i> = ...</p>	

Carbon, Nitrogen, Phosphorus and Silica: aed_carbon, aed_nitrogen, aed_phosphorus, aed_silica, aed_organic_matter

Both the inorganic and organic, and dissolved and particulate forms of C, N and P are modelled explicitly along the degradation pathway of POM to DOM to dissolved inorganic matter (DIM). The decomposition and mineralisation process varies in response to temperature, and is additionally able to slow down under anaerobic conditions. The nitrogen cycle includes the additional processes of denitrification, nitrification and N₂ fixation (discussed in the phytoplankton section) that are not in the carbon and phosphorus cycles, though note N₂ levels are not tracked as a state variable. The phosphorus cycle also accounts for adsorption/desorption of PO₄ onto suspended solids (SS), and adopts the Langmuir isotherm model as implemented by Chao et al. (2010).

The silica cycle is simpler and includes the processes of biological uptake of dissolved Si (RSi) by diatoms into the internal Si (ISi) pool, dissolved sediment fluxes of RSi, diatom mortality directly into the RSi sediment pool, settling of ISi. This relatively simple representation assumes that diatom frustules rapidly mineralize.

Table 4: Mass balance and functions related to silica cycling.

<u>State variable mass balance equations:</u>	
$\frac{dRSi}{dt} = +f_{sed}^{RSi} - \sum_a^{N_{PHY}} f_{uptake}^{PHY-Si_a} + \sum_a^{N_{PHY}} f_{excr}^{PHY-Si_a}$	= ± sediment flux – uptake by phytoplankton groups – excretion by phytoplankton groups
<i>PHY_{Si}</i> is also included in the Si cycle and described in the phytoplankton module	
<u>Process parameterisations:</u>	
$f_{sed}^{O_2} = F_{max}^{O_2} \frac{O_2}{K_{sed}^{O_2} + O_2} \left(\theta_{sed}^{O_2} \right)^{T-20} \left(\frac{\widehat{A}_z}{dz_z} \right)$	sediment reactive Si flux
where $\widehat{A}_z = A_z^{ben} / A_z$ and dz_z is the thickness of the z^{th} layer/cell.	

Table 5: Mass balance and functions related to carbon cycling.

<p><u>State variable mass balance equations:</u></p> $\frac{dCH_4}{dt} = +f_{sed}^{CH_4} - f_{ox}^{CH_4}$ <ul style="list-style-type: none"> = ± sediment flux - oxidation to DIC $\frac{dDIC}{dt} = f_{miner}^{DOC} + f_{sed}^{DIC} + \sum_a^{N_{PHY}} [f_{resp}^{PHY_{Ca}} - f_{uptake}^{PHY_{Ca}}] + \sum_z^{N_{ZOO}} f_{resp}^z$ <ul style="list-style-type: none"> = + respiration by bacteria during DOM breakdown ± sediment flux ± carbon fixation and respiration by phytoplankton groups + respiration by zooplankton groups $\frac{dDOC}{dt} = f_{decom}^{POC} - f_{miner}^{DOC} + f_{sed}^{DOC} + \sum_a^{N_{PHY}} f_{excr}^{PHY_{Ca}} + \sum_z^{N_{ZOO}} f_{excr}^z$ <ul style="list-style-type: none"> = + decomposition from particulate detritus (POC) - mineralisation by bacteria ± sediment flux - excretion by phytoplankton groups - excretion by zooplankton groups $\frac{dPOC}{dt} = -f_{decom}^{POC} - f_{sett}^{POC} + \sum_a^{N_{PHY}} f_{mort}^{PHY_{Ci}} + \sum_z^{N_{ZOO}} [(1 - k_{assim}^z) f_{assim}^z + (1 - k_{fsed}^z) f_{fecal}^z + f_{mort}^z]$ <ul style="list-style-type: none"> = - decomposition to DOC ± sedimentation + mortality from phytoplankton groups + messy feeding, faecal pellet release and mortality from zooplankton groups 	
<p>PHY_N and ZOO_N are described in the phytoplankton and zooplankton sub-sections.</p>	
<p><u>Process parameterisations:</u></p> $f_{sett}^{POC} = \frac{\omega_{POC}}{dz_z} [POC]$ <p style="text-align: right;">sedimentation of particulate organic carbon</p> $f_{decom}^{POC} = R_{decom}^{POC} \frac{[O_2]}{K_{miner} + [O_2]} (\theta_{decom})^{T-20} [POC]$ <p style="text-align: right;">hydrolysis/decomposition of POC</p> $f_{miner}^{DOC} = R_{miner}^{DOC} \frac{[O_2]}{K_{miner} + [O_2]} (\theta_{miner})^{T-20} [DOC]$ <p style="text-align: right;">mineralisation of DOC</p> $f_{sed}^{DOC} = F_{max}^{DOC} \frac{K_{sed}^{DOC}}{K_{sed}^{DOC} + [DOC]} (\theta_{sed}^{DOC})^{T-20} \left(\frac{\widehat{A}_z}{dz_z} \right)$ <p style="text-align: right;">DOC sediment flux</p>	
<p>where $\widehat{A}_z = A_z^{ben}/A_z$ and dz_z is the thickness of the z^{th} layer/cell.</p>	
<p><u>Diagnostic & derived outputs:</u></p> <p>pH</p> <p>$pH = -\log [H^+]$, where H^+ is determined based on the carbonate alkalinity (CA) and DIC concentrations.</p> <p>Total Organic Carbon</p>	

$$TOC = DOC + POC + \sum_a^{N_{PHY}} PHY_{Ca} + \sum_z^{N_{ZOO}} ZOO_z$$

note: if multiple POC/DOC pools are simulated then these can be included in TOC through the aed_totals routine.

Table 6: Mass balance and functions related to nitrogen cycling.

<u>State variable mass balance equations:</u>	
$\frac{dNH_4}{dt} = +f_{sed}^{NH_4} + f_{miner}^{DON} - f_{nitrif}^{NH_4} - \sum_a^{N_{PHY}} [p_{NH_4}^a \times f_{uptake}^{PHY-Na}]$	= ± sediment flux + mineralization from DON - nitrification - uptake from the phytoplankton community
$\frac{dNO_3}{dt} = -f_{sed}^{NO_3} + f_{nitrif}^{NH_4} - f_{denit}^{NO_3} - \sum_a^{N_{PHY}} [p_{NO_3}^a \times f_{uptake}^{PHY-Na}]$	= ± sediment flux + nitrification - denitrification - uptake from the phytoplankton community
$\frac{dDON}{dt} = +f_{decom}^{PON} + f_{sed}^{DON} - f_{miner}^{DON} + \sum_a^{N_{PHY}} f_{excr}^{PHY-Na} + \sum_z^{N_{ZOO}} \frac{f_{excr}^z}{\chi_{C:N}^z}$	= + decomposition from particulate detritus (POC) - mineralisation by bacteria ± sediment flux - excretion by phytoplankton groups - excretion by zooplankton groups
$\frac{dPON}{dt} = -f_{decom}^{PON} - f_{sett}^{PON} + \sum_i^{N_{PHY}} f_{mort}^{PHY-Na} + \sum_z^{N_{ZOO}} [(1 - k_{assim}^z) f_{assim}^z + (1 - k_{fsed}^z) f_{fecal}^z + f_{mort}^z] \frac{1}{\chi_{C:N}^z}$	= - decomposition to DOC ± sedimentation + mortality from phytoplankton groups + messy feeding, faecal pellet release and mortality from zooplankton groups
<i>PHY_N</i> and <i>ZOO_N</i> are described in the phytoplankton and zooplankton sub-sections.	
<u>Process parameterisations:</u>	
$f_{sed}^{NH_4} = F_{max}^{NH_4} \frac{K_{sed}^{NH_4}}{K_{sed}^{NH_4} + [O_2]} (\theta_{sed}^{NH_4})^{T-20} \left(\frac{\widehat{A}_z}{dz_z} \right)$	ammonium sediment flux
$f_{sed}^{NO_3} = F_{max}^{NO_3} \frac{[O_2]}{K_{sed}^{NO_3} + [O_2]} (\theta_{sed}^{NO_3})^{T-20} \left(\frac{\widehat{A}_z}{dz_z} \right)$	nitrate sediment flux
$f_{sed}^{DON} = F_{max}^{DON} \frac{K_{sed}^{DON}}{K_{sed}^{DON} + [DON]} (\theta_{sed}^{DON})^{T-20} \left(\frac{\widehat{A}_z}{dz_z} \right)$	DON sediment flux
$f_{sett}^{PON} = \frac{\omega_{PON}}{dz_z} [PON]$	sedimentation of particulate organic nitrogen
$f_{sett}^{PHY-Ni} = \frac{\omega_{PHY_i}}{dz_z} [PHY-Na]$	sedimentation of phytoplankton
$f_{decom}^{PON} = R_{decom}^{PON} \frac{[O_2]}{K_{miner} + [O_2]} (\theta_{decom})^{T-20} [PON]$	hydrolysis/decomposition of PON

$$f_{miner}^{DON} = R_{miner}^{DON} \frac{[O_2]}{K_{miner}+[O_2]} (\theta_{miner})^{T-20} [DON] \quad \text{mineralisation of DON}$$

$$f_{nitrif}^{NH_4} = R_{nitrif} \frac{[O_2]}{K_{nitrif}+[O_2]} (\theta_{nitrif})^{T-20} [NH_4] \quad \text{nitrification}$$

$$f_{denit}^{NO_3} = R_{denit} \frac{K_{denit}}{K_{denit}+[O_2]} (\theta_{denit})^{T-20} [NO_3] \quad \text{denitrification}$$

where $\widehat{A}_z = A_z^{ben}/A_z$ and dz_z is the thickness of the z^{th} layer/cell.

Diagnostic & derived outputs:

Total Nitrogen

$$TN = NO_3 + NH_4 + DON + PON + \sum_a^{N_{PHY}} PHY_{Na} + \sum_z^{N_{ZOO}} \frac{ZOO_z}{\chi_{C:N}^z}$$

Total Kjeldahl Nitrogen

$$TKN = NH_4 + DON + PON + \sum_a^{N_{PHY}} PHY_{Na} + \sum_z^{N_{ZOO}} \frac{ZOO_z}{\chi_{C:N}^z}$$

note: if multiple PON/DON pools are simulated then these can be included in TN through the aed_totals routine.

Table 7: Mass balance and functions related to phosphorus cycling.

<u>State variable mass balance equations:</u>	
$\frac{dPO_4}{dt} = +f_{sed}^{PO_4} + f_{miner}^{DOP} \pm f_{ads}^{PO_4} - \sum_a^{N_{PHY}} [f_{uptake}^{PHY-Pa}]$	<ul style="list-style-type: none"> = ± sediment flux + mineralization from DOP ± adsorption/desorption - uptake from the phytoplankton community
$\frac{dPO_4^{ads}}{dt} = \pm f_{ads}^{PO_4} - f_{sett}^{PO_4^{ads}}$	<ul style="list-style-type: none"> = ± adsorption/desorption ± sedimentation
$\frac{dPOP}{dt} = -f_{decom}^{POP} - f_{sett}^{POP} + \sum_a^{N_{PHY}} f_{mort}^{PHY-Pa} + \sum_z^{N_{ZOO}} [(1 - k_{assim}^z) f_{assim}^z + (1 - k_{fsed}^z) f_{fecal}^z + f_{mort}^z] \frac{1}{\chi_{C:P}^z}$	<ul style="list-style-type: none"> = - decomposition to DOP ± sedimentation + mortality from phytoplankton groups + messy feeding, faecal pellet release and mortality from zooplankton groups
$\frac{dDOP}{dt} = f_{decom}^{POP} - f_{miner}^{DOP} + f_{sed}^{DOP} + \sum_a^{N_{PHY}} f_{excr}^{PHY-Pa} + \sum_z^{N_{ZOO}} 1/\chi_{C:P}^z f_{excr}^z$	<ul style="list-style-type: none"> = + decomposition from particulate detritus (POP) - mineralisation by bacteria ± sediment flux - excretion by phytoplankton groups - excretion by zooplankton groups
PHY _P and ZOO _P are described in the phytoplankton and zooplankton sub-sections.	
<u>Process parameterisations:</u>	
$f_{sed}^{PO_4} = F_{max}^{PO_4} \frac{K_{sed}^{PO_4}}{K_{sed}^{PO_4} + [O_2]} (\theta_{sed}^{PO_4})^{T-20} \left(\frac{\widehat{A}_z}{dz_z} \right)$	phosphate sediment flux
$f_{sed}^{DOP} = F_{max}^{DOP} \frac{K_{sed}^{DOP}}{K_{sed}^{DOP} + [DOP]} (\theta_{sed}^{DOP})^{T-20} \left(\frac{\widehat{A}_z}{dz_z} \right)$	dissolved organic phosphorus sediment flux
$f_{sett}^{POP} = \frac{\omega_{POP}}{dz_z} [POP]$	sedimentation of particulate organic phosphorus
$f_{sett}^{PHY-Pa} = \frac{\omega_{PHYa}}{dz_z} [PHY-Pa]$	sedimentation of phytoplankton
$f_{sett}^{PO_4^{ads}} = \frac{\omega_{SS}}{dz_z} [PO_4^{ads}]$	sedimentation of adsorbed phosphorus
$f_{ads}^{PO_4} = [\Phi_{ads}^{PO_4}([TPO_4]^{t+1}, SS, pH) \times [TPO_4]^{t+1} - PO_4^{ads*}] \frac{1}{\Delta t}$	adsorption/desorption 'rate' of phosphorus

$$\Phi_{ads}^{PO_4}(TPO_4, SS, pH) = \frac{1}{2IP} \left[\left(TPO_4 + \frac{1}{c_{ads}^r} + c_{ads}^{max} \Phi_{ads}^{pH}(pH) SS \right) - \sqrt{\left(TPO_4 + \frac{1}{c_{ads}^r} + c_{ads}^{max} \Phi_{ads}^{pH}(pH) SS \right)^2 + \frac{4c_{ads}^{max} \Phi_{ads}^{pH}(pH)}{c_{ads}^r} SS} \right]$$

adsorbed fraction of total available inorganic phosphorus

where $\widehat{A}_z = A_z^{ben}/A_z$ and dz_z is the thickness of the z^{th} layer/cell.

Diagnostic & derived outputs:

Total Phosphorus

$$TP = PO_4 + PO_4^{ads} + DOP + POP + \sum_a^{N_{PHY}} PHY_{P_a} + \sum_z^{N_{ZOO}} \frac{ZOO_z}{\chi_{C:P}^z}$$

Total Inorganic Phosphate

$$TPO_4 = PO_4 + PO_4^{ads}$$

note: if multiple POP/DOP pools are simulated then these can be included in TN through the aed_totals routine.

Phytoplankton Dynamics – aed_phytoplankton

Each phytoplankton group configurable within the AED phytoplankton module is generic, and can include internal nitrogen, phosphorus and/or silica stores if desired. The algal biomass of each group, PHY_C , is simulated in units of carbon (mmol C m⁻³), and the group can be configured to have a constant C:N:P:Si ratio, or have dynamic uptake of N and P sources in response to changing water column condition and cellular physiology.

Balance equations for the phytoplankton related state variables are in Table 8.

Table 8: Mass balance and functions related to the phytoplankton model.

<u>State variable mass balance equations:</u>	
Carbon	$\frac{d(PHY_{C,a})}{dt} = +f_{uptake}^{PHY_{C,a}} - f_{excr}^{PHY_{C,a}} - f_{mort}^{PHY_{C,a}} - f_{resp}^{PHY_{C,a}} - f_{sett}^{PHY_{C,a}} - \sum_z^{N_{ZOO}} (f_{assim}^z p_a^z)$
Nitrogen	$\frac{d(PHY_{N,a})}{dt} = +f_{uptake}^{PHY_{N,a}} - f_{excr}^{PHY_{N,a}} - f_{mort}^{PHY_{N,a}} - f_{sett}^{PHY_{N,a}} - \sum_z^{N_{ZOO}} \left(f_{assim}^z p_a^z \frac{PHY_{N,a}}{PHY_{C,a}} \right)$
Phosphorus	$\frac{d(PHY_{P,a})}{dt} = +f_{uptake}^{PHY_{P,a}} - f_{excr}^{PHY_{P,a}} - f_{mort}^{PHY_{P,a}} - f_{sett}^{PHY_{P,a}} - \sum_z^{N_{ZOO}} \left(f_{assim}^z p_a^z \frac{PHY_{P,a}}{PHY_{C,a}} \right)$
Silica	$\frac{d(PHY_{Si,a})}{dt} = +f_{uptake}^{PHY_{Si,a}} - f_{excr}^{PHY_{Si,a}} - f_{sett}^{PHY_{Si,a}} - \sum_z^{N_{ZOO}} \left(f_{assim}^z p_a^z \frac{PHY_{Si,a}}{PHY_{C,a}} \right)$ <ul style="list-style-type: none"> = + uptake (C,N,P & Si) - excretion - mortality - vertical movement (settling or migration) - grazing
<u>Diagnostic & derived outputs:</u>	
Chlorophyll-a	$TCHLA = \sum_a^{N_{PHY}} \left\{ \chi_{C:Chla}^{PHY_a} PHY_{C,a} \right\}$
Gross-primary production	$GPP = \sum_a^{N_{PHY}} \left\{ \chi_{C:Chla}^{PHY_a} PHY_{C,a} \right\}$

Process summary: Photosynthesis and nutrient uptake

For each phytoplankton group, the maximum potential growth rate at 20°C is multiplied by the minimum value of expressions for limitation by light, phosphorus, nitrogen and silica (when configured). While there may be some interaction between limiting factors, a minimum expression is likely to provide a realistic representation of growth limitation (Rhee and Gotham, 1981).

Therefore, photosynthesis is parameterized as the uptake of carbon, and depends on the temperature, light and nutrient dimensionless functions (adopted from Hipsey & Hamilton, 2008; Li *et al.*, 2013).

$$f_{\text{uptake}}^{\text{PHY}_{C_a}} = \underbrace{R_{\text{growth}}^{\text{PHY}_a}}_{\substack{\text{max growth} \\ \text{rate at } 20\text{C}}} \underbrace{(1 - k_{pr}^{\text{PHY}_a})}_{\text{photorespiratory loss}} \underbrace{\Phi_{\text{tem}}^{\text{PHY}_a}(T)}_{\text{temperature scaling}} \underbrace{\Phi_{\text{str}}^{\text{PHY}_a}(T)}_{\text{metabolic stress}} \dots \\ \dots \min \left\{ \underbrace{\Phi_{\text{light}}^{\text{PHY}_a}(I)}_{\text{light limitation}}, \underbrace{\Phi_N^{\text{PHY}_a}(NO_3, NH_4, \text{PHY}_{N_a})}_{\text{N limitation}}, \underbrace{\Phi_P^{\text{PHY}_a}(PO_4, \text{PHY}_{P_a})}_{\text{P limitation}}, \underbrace{\Phi_{Si}^{\text{PHY}_a}(RSi)}_{\text{Si limitation}} \right\} [\text{PHY}_{C_a}]$$

To allow for reduced growth at non-optimal temperatures, a temperature function is used where the maximum productivity occurs at a temperature T_{OPT} ; above this productivity decreases to zero at the maximum allowable temperature, T_{MAX} . Below the standard temperature, T_{STD} the productivity follows a simple Arrhenius scaling formulation. In order to fit a function with these restrictions the following conditions are assumed: at $T = T_{STD}$, $\Phi_{\text{tem}}(T) = 1$ and at $T = T_{OPT}$, $\frac{d\Phi_{\text{tem}}(T)}{dT} = 0$, and at $T = T_{MAX}$, $\Phi_{\text{tem}}(T) = 0$. This can be numerically solved using Newton's iterative method and can be specific for each phytoplankton group. The temperature function is calculated according to (Griffin *et al.* 2001):

$$\Phi_{\text{tem}}^{\text{PHY}_a}(T) = \vartheta_a^{T-20} - \vartheta_a^{k[T-c1_a]} + c0_a$$

where $c1_a$ and $c0_a$ are solved numerically given input values of: T_a^{std} , T_a^{opt} and T_a^{max} .

The level of light limitation on phytoplankton growth can be modelled as photoinhibition or non-photoinhibition. In the absence of significant photoinhibition, Webb *et al.* (1974) suggested a relationship for the fractional limitation of the maximum potential rate of carbon fixation for the case where light saturation behavior was absent (Talling, 1957), and the equations can be analytically integrated with respect to depth (Hipsey and Hamilton, 2008). For the case of photoinhibition, the light saturation value of maximum production (I_s) is used and the net level effect can be averaged over the cell by integrating over depth.

The `aed_phytoplankton` module contains several light functions, including those from a recent review by Baklouti *et al.* (2006). The user must select the sensitivity to light according to a photosynthesis-irradiance (P-I curve) formulation and each species must be set to be either non-photoinhibited or photoinhibited according to the options in Table 9.

Table 9: Selection of P-I functions available for selection for each species in aed_phytoplankton.

$\Phi_{light}^{PHY_a}(I) =$				
$1 - e^{\left(-\frac{I}{I_{K_a}}\right)}$	$\Theta_{Light}^{PHY_a} = 0$	Non-photoinhibited		Webb et al. (1974), with numerical integration over depth as in CAEDYM (Hipsey and Hamilton, 2008)
$\frac{\left(\frac{I}{I_{K_a}}\right)}{1 + \left(\frac{I}{I_{K_a}}\right)}$	$\Theta_{Light}^{PHY_a} = 1$	Non-photoinhibited		Monod (1950)
$\frac{I}{I_{S_a}} e^{\left(1 - \frac{I}{I_{S_a}}\right)}$	$\Theta_{Light}^{PHY_a} = 2$	Photoinhibited		Steele (1962)
$1 - e^{\left(-\frac{I}{I_{K_a}}\right)}$	$\Theta_{Light}^{PHY_a} = 3$	Non-photoinhibited		Webb et al. (1974)
$\tanh\left(\frac{I}{I_{K_a}}\right)$	$\Theta_{Light}^{PHY_a} = 4$	Non-photoinhibited		Jassby and Platt (1976)
$\frac{e^{\left(\frac{I}{I_{K_a}} + \epsilon\right)} - 1}{e^{\left(\frac{I}{I_{K_a}} + \epsilon\right)} + \epsilon}$	$\Theta_{Light}^{PHY_a} = 5$	Non-photoinhibited		Chalker (1980); $\epsilon \sim 0.5$
$\frac{(2 + A)\left(\frac{I}{I_{S_a}}\right)}{1 + A\left(\frac{I}{I_{S_a}}\right) + \left(\frac{I}{I_{S_a}}\right)^2}$	$\Theta_{Light}^{PHY_a} = 6$	Photoinhibited		Klepper et al. (1988); $A \sim 5$.

Limitation of the photosynthetic rate may be dampened according to nitrogen or phosphorus availability, and this is either approximated using a Monod expression of the static model is chosen, or based on the internal nutrient stoichiometry if the dynamic (Droop uptake) model is selected:

For advanced users, an optional metabolic scaling factor can be included to reduce the photosynthetic capacity of the simulated organisms, for example due to metabolic stress due to undertaking N₂ fixation:

$$\Phi_{str}^{PHY_a} = \underbrace{f_{NF}^{PHY_a} + [1 - f_{NF}^{PHY_a}] \Phi_N^{PHY_a}(NO_3, NH_4, PHY_{N_a})}_{N_2 \text{ fixation growth scaling}}$$

The above discussion relates to photosynthesis and carbon uptake by the phytoplankton community. In addition users must choose one of two options to model the P, N uptake dynamics for each algal group: a constant nutrient to carbon ratio, or dynamic intracellular stores. For the first model a simple Michaelis-Menten equation is used to model nutrient limitation with a half-saturation constant for the effect of external nutrient concentrations on the growth rate.

The internal phosphorus and nitrogen dynamics within the phytoplankton groups can be modelled using dynamic intracellular stores that are able to regulate growth based on the model of Droop (1974). This model allows for the phytoplankton to have dynamic nutrient uptake rates with variable internal nutrient concentrations bounded by user-defined minimum and maximum values (e.g., see Li *et al.*, 2013).

Table 10: N, P and Si phytoplankton uptake rate functions.

$f_{uptake}^{PHY_N_a}$				
$f_{uptake}^{PHY_Ca} / \chi_{C:N}^{PHY_a}$	$\Theta_{NUptake}^{PHY_a} = 0,1$	Static uptake rate	-	
$R_{NUptake}^{PHY_a} \Phi_{tem}^{PHY_a}(T) \left\{ \Phi_N^{PHY_a} \frac{\left(\frac{[PHY_N_a]}{[PHY_{Ca}]} - \chi_{NMIN}^{PHY_a} \right)}{(\chi_{NMAX}^{PHY_a} - \chi_{NMIN}^{PHY_a})} \right\} [PHY_N_a]$	$\Theta_{NUptake}^{PHY_a} = 2$	Dynamic uptake rate	Hipsey and Hamilton (2008)	
$f_{uptake}^{PHY_P_a}$				
$f_{uptake}^{PHY_Ca} / \chi_{C:P}^{PHY_a}$	$\Theta_{PUpTake}^{PHY_a} = 0,1$	Static uptake rate	-	
$R_{PUpTake}^{PHY_a} \Phi_{tem}^{PHY_a}(T) \left\{ \Phi_P^{PHY_a} \frac{\left(\frac{[PHY_P_a]}{[PHY_{Ca}]} - \chi_{PMIN}^{PHY_a} \right)}{(\chi_{PMAX}^{PHY_a} - \chi_{PMIN}^{PHY_a})} \right\} [PHY_P_a]$	$\Theta_{PUpTake}^{PHY_a} = 2$	Dynamic uptake rate	Hipsey and Hamilton (2008)	
$f_{uptake}^{PHY_{Si_a}}$				
$f_{uptake}^{PHY_Ca} / \chi_{C:Si}^{PHY_a}$		Static uptake rate	-	

The uptake of nitrogen must be partitioned into uptake of NO₃, NH₄ and potentially labile DON. In the present version, distinction between uptake of NO₃ and NH₄ is calculated automatically via a preference factor:

$$p_{NH4}^{PHY_a} = \frac{NO_3 \text{NH}_4}{(NH_4 + K_N^{PHY_a})(NO_3 + K_N^{PHY_a})} \frac{NH_4 K_N^{PHY_a}}{(NH_4 + NO_3)(NO_3 + K_N^{PHY_a})}$$

$$p_{NO3}^{PHY_a} = 1 - p_{NH4}^{PHY_a}$$

For diatom groups, silica processes are simulated that include uptake of dissolved silica. The silica limitation function for diatoms is similar to the constant cases for nitrogen and phosphorus which assumes a fixed C:Si ratio.

Process summary: Respiration, excretion and mortality

Metabolic loss of nutrients from mortality and excretion is proportional to the internal nitrogen to chla ratio multiplied by the loss rate and the fraction of excretion and mortality that returns to the detrital pool. Loss terms for respiration, natural mortality and excretion are modelled with a single 'respiration' rate coefficient. This loss rate is then divided into the pure respiratory fraction and losses due to mortality and excretion. The constant f_{DOM} is the fraction of mortality and excretion to the dissolved organic pool with the remainder into the particulate organic pool.

Nutrient losses through mortality and excretion for the internal nutrient model are similar to the simple model described above, except that dynamically calculated internal nutrient concentrations are used.

$$\hat{R} = R_{resp}^{PHY_a} \Phi_{sal}^{PHY_a}(S) (\vartheta_{resp}^{PHY_a})^{T-20}$$

$$f_{resp}^{PHY_Ca} = k_{fres}^{PHY_a} \hat{R} [PHY_{C_a}]$$

$$f_{excr}^{PHY_Ca} = (1 - k_{fres}^{PHY_a}) k_{fdom}^{PHY_a} \hat{R} [PHY_{C_a}]$$

$$f_{mort}^{PHY_Ca} = (1 - k_{fres}^{PHY_a}) (1 - k_{fdom}^{PHY_a}) \hat{R} [PHY_{C_a}]$$

$$f_{excr}^{PHY_Na} = k_{fdom}^{PHY_a} \hat{R} [PHY_{N_a}]$$

$$f_{mort}^{PHY_Na} = (1 - k_{fdom}^{PHY_a}) \hat{R} [PHY_{N_a}]$$

$$f_{excr}^{PHY_Pa} = k_{fdom}^{PHY_a} \hat{R} [PHY_{P_a}]$$

$$f_{mort}^{PHY_Pa} = (1 - k_{fdom}^{PHY_a}) \hat{R} [PHY_{P_a}]$$

$$f_{excr}^{PHY_{Si}a} = \hat{R} [PHY_{Si_a}]$$

The salinity effect on mortality is given by various quadratic formulations, depending on the groups sensitivity to salinity (Griffin et al 2001; Robson and Hamilton, 2004). An example of the use of various salinity limitation options is shown in Figure 3.

Table 11: Respiration multiplier as a function of salinity.

$\Phi_{sal}^{PHY_a}(S) =$			
1		$\Theta_{SalTol}^{PHY_a} = 0$	No salinity effect
$\begin{cases} 1 & \text{if } S < S_{opt}^{PHY_a} \\ 1 + \frac{(S_{bep}^{PHY_a} - 1) S^2}{(S_{max}^{PHY_a} - S_{opt}^{PHY_a})^2} - \frac{2(S_{bep}^{PHY_a} - 1) S_{opt}^{PHY_a} S}{(S_{max}^{PHY_a} - S_{opt}^{PHY_a})^2} + \frac{(S_{bep}^{PHY_a} - 1)(S_{opt}^{PHY_a})^2}{(S_{max}^{PHY_a} - S_{opt}^{PHY_a})^2} & \text{if } S > S_{opt}^{PHY_a} \end{cases}$	$\Theta_{SalTol}^{PHY_a} = 1$	Freshwater species	
$\begin{cases} 1 & \text{if } S < S_{opt}^{PHY_a} \\ \frac{(S_{bep}^{PHY_a} - 1) S^2}{(S_{opt}^{PHY_a})^2} - \frac{2(S_{bep}^{PHY_a} - 1) S}{(S_{opt}^{PHY_a})^2} & \text{if } S > S_{opt}^{PHY_a} \end{cases}$		$\Theta_{SalTol}^{PHY_a} = 2$	Marine species
$\begin{cases} 1 & \text{if } S < S_{opt}^{PHY_a} \\ S_{bep}^{PHY_a} + \frac{(S_{bep}^{PHY_a} - 1) S^2}{(S_{opt}^{PHY_a})^2} - \frac{2(S_{bep}^{PHY_a} - 1) S}{(S_{opt}^{PHY_a})^2} & \text{if } S > S_{opt}^{PHY_a} \end{cases}$		$\Theta_{SalTol}^{PHY_a} = 3$	Estuarine species

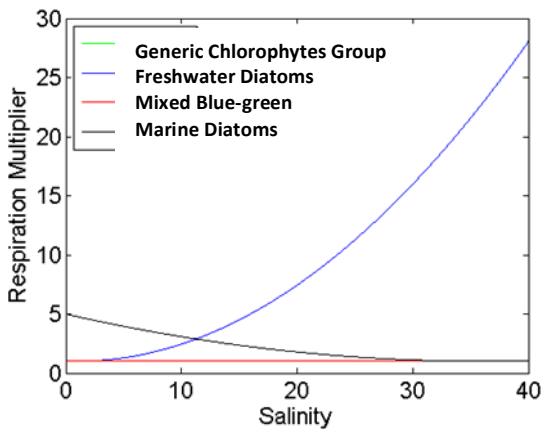


Figure 3: Example salinity response functions, $\Phi_{sal}^{PHY}(S)$, for four phytoplankton groups being simulated within a river-estuary model. This example demonstrates how fresh, estuarine and marine species can be incorporated together.

Zooplankton Dynamics – aed_zooplankton

Net zooplankton growth is calculated as a balance between food assimilation and losses from respiration, excretion, egestion, predation and mortality. Food assimilation is calculated as the product of the maximum potential rate of grazing, assimilation efficiency and temperature and food limitation functions. A constant internal nutrient ratio is assumed for simplicity, and since the various input and output fluxes have variable C:N:P ratios, the excretion of nutrients is dynamically adjusted each time-step to maintain this ratio at each time step.

Table 12: Zooplankton balance equations .

<u>State variable mass balance equations:</u>	
$\frac{d(ZOO_z)}{dt} = k_{assim}^z \times f_{assim}^z - f_{loss}^z - f_{mort}^z$	= + carbon and nutrient assimilation from grazing various ecosystem pools - carbon loss via respiration - excretion of DOM - faecal pellet production - mortality - predation by larger organisms
ZOO_N and ZOO_P are not dynamically solved but set at a constant ratio to zooplankton carbon.	
<u>Process parameterisations:</u>	
$f_{assim}^z = R_{grz}^{ZOO P} \Phi_{tem}^z(T) [ZOO]$	zooplankton assimilation
$f_{loss}^z = R_{loss}^{ZOO P} (\theta_{loss}^z)^{T-20} [ZOO]$	zooplankton loss
$f_{excr}^z = k_{excr}^z \times f_{loss}^z$	zooplankton excretion
$f_{fecal}^z = k_{fecal}^z \times f_{loss}^z$	zooplankton fecal pellets
$f_{mort}^z = R_{mort}^z \Phi_{sal}^z(S) \times (\theta_{loss}^z)^{T-20} [ZOO]$	zooplankton mortality

Suspended Sediment & Turbidity : aed_tracer, aed_totals

Modellers can use the aed_tracer to simulate a particulate tracer that can be set to also settle and decay. In addition to suspended sediment simulated in this way, the aed_totals module has an option to assign any number of FABM variables (including non-AED variables) to contribute to a turbidity, subject to a transformation coefficient.

Geochemical Dynamics : aed_geochemistry, aed_iron, aed_sulfur

The Oct 2013 release of AED with GLM v1.3.2 contains several geochemistry modules - documentation for these modules is pending.

Sediment Biogeochemistry – aed_sedflux, aed_seddiagenesis

The AED modules has aimed to provide flexibility in how users may want to simulate sediment-water interaction. This includes a simple flux equation, or a simple mass balance model maintains a mass balance of C, N, P, Si, DO and SS in both the water column and a single sediment layer. At this development stage only sufficient complexity is implemented in the sediments to maintain mass conservation. The sediment fluxes of dissolved inorganic and organic nutrients are based on empirical formulations that account for environmental sensitivities and require laboratory and field studies to establish parameter values. Resuspension of particulate nutrients is currently not configured, however note that the resuspension of inorganic sediments is performed through the TUFLOW-FV driver.

The Oct 2013 release of AED contains a more detailed sediment diagenesis model that includes vertical resolution - documentation for this module is pending.

Pathogens – aed_pathogens

The pathogen module is a reimplementation of Hipsey et al. (2008). Users are referred to this paper for details of simulatable variables, process parameterisations and parameter values.

Parameter summary

This section summarises the parameters introduced in the previous section with some comments and references to help those new to the model get started. Please note that the process of parameter estimation in aquatic ecosystem models is highly complex and this summary is by no means an exhaustive review of relevant parameter values, and applying these values may not lead to an acceptable validation.

Below Table 9 summarises sediment related parameters, Table 10 summarises biogeochemical parameters relevant to nutrient cycling, and Table 11 and 12 summarise phytoplankton and zooplankton parameters respectively.

Note that in collaboration with the Aquatic Ecological Modelling Network (AEMON), a more detailed database of species parameters is being developed which may be referred to search for specific parameters for a given species, or to see typical values for functional groups used in other modelling studies:

<https://sites.google.com/site/aquaticmodelling/>

Click on *Resources* and then follow the link to "*Parameter database*"

Table 13: Summary of sediment parameter descriptions, units and typical values.

Symbol	Description	Units	Default value	Comment
$F_{max}^{O_2}$	maximum flux of oxygen across the sediment water interface into the sediment	mmol O ₂ /m ² /d	48.0	Lake: 6 – 38 ^A River: 9.4 – 20.3 ^B Estuary: 48 ^C ; 79 ^D ; ~50 ^E
$K_{sed}^{O_2}$	half saturation constant for oxygen dependence of sediment oxygen flux	mmol O ₂ /m ³	150	Lake: 15.6 ^A Estuary: 150 ^C ; ~50 ^F
$\theta_{sed}^{O_2}$	temperature multiplier for temperature dependence of sediment oxygen flux	-	= θ_{sed} = 1.08	1.04 – 1.10 ^A
F_{max}^{RSi}	maximum flux of silica across the sediment water interface	mmol Si/m ² /d	4	Lake: 0.6 ^A Estuary: 4 – 40 ^E
K_{sed}^{RSi}	half saturation constant for oxygen dependence of sediment silica flux	mmol Si/m ³	150	estimated
θ_{sed}^{RSi}	temperature multiplier for temperature dependence of sediment silica flux	-	= θ_{sed} = 1.08	1.04 – 1.10 ^A
$F_{max}^{PO_4}$	maximum flux of phosphate across the sediment water interface	mmol P/m ² /d	0.2	Lake: 0.080 – 0.125 ^A River: 0.0 – 0.10 ^B Estuary: 0.3 – 4 ^E
$K_{sed}^{PO_4}$	half saturation constant for oxygen dependence of sediment phosphate flux	mmol O ₂ /m ³	20	Lake: 15.6 ^{A, J} Estuary: >200 ^F
$\theta_{sed}^{PO_4}$	temperature multiplier for temperature dependence of sediment phosphate flux	-	= θ_{sed} = 1.08	1.04 – 1.10 ^A
F_{max}^{DOP}	maximum flux of dissolved organic phosphorus across the sediment water interface	mmol P/m ² /d	0.05	Lake: 0.03 ^A River: 0.05 – 0.10 ^B
K_{sed}^{DOP}	half saturation constant for oxygen dependence of sediment dissolved organic phosphorus flux	mmol O ₂ /m ³	150	estimated
θ_{sed}^{DOP}	temperature multiplier for temperature dependence of sediment dissolved organic phosphorus flux	-	= θ_{sed} = 1.08	1.04 – 1.10 ^A
$F_{max}^{NH_4}$	maximum flux of ammonium across the sediment water interface	mmol N/m ² /d	30.0	Lake: 1.35 – 6.42 ^A River: 4.3 – 12.8 ^B Estuary: 30 ^C ; 5 – 25 ^E
$K_{sed}^{NH_4}$	half saturation constant for oxygen dependence of sediment ammonium flux	mmol N/m ³	31.25	Lake: 1.56 – 15.6 ^A Estuary: 31.25 ^C
$\theta_{sed}^{NH_4}$	temperature multiplier for temperature dependence of sediment ammonium flux	-	1.08	1.04 – 1.10 ^A
$F_{max}^{NO_3}$	maximum flux of nitrate across the sediment water interface	mmol N/m ² /d	5.2	Lake: -21.4 – -7.14 ^A River: 4.3 – 12.8 ^B Estuary: 5.2 ^C ; -7.2 – 7.1 ^E
$K_{sed}^{NO_3}$	half saturation constant for oxygen dependence of sediment nitrate flux	mmol O ₂ /m ³	100.0	Lake: 2.14 – 15.6 ^A Estuary: 100 ^C
$\theta_{sed}^{NO_3}$	temperature multiplier for temperature dependence of sediment nitrate flux	-	= θ_{sed} = 1.08	1.04 – 1.10 ^A
F_{max}^{DON}	maximum flux of dissolved organic nitrogen across the sediment water interface	mmol N/m ² /d	5.2	Lake: 0.07 – 0.57 ^A River: 1.28 – 2.20 ^B
K_{sed}^{DON}	half saturation constant for oxygen dependence of sediment dissolved organic nitrogen flux	mmol N/m ³	100.0	estimated
θ_{sed}^{DON}	temperature multiplier for temperature dependence of sediment dissolved organic nitrogen flux	-	= θ_{sed} = 1.08	1.04 – 1.10 ^A

^A Converted from data on oligotrophic lakes (Romero et al. 2004) to eutrophic lakes (Gal et al. 2009), and justifications therein.

^B Based on Hipsey et al. (2010) ELCOM-CAEDYM model of the lower Murray River; estimated from field data from Justin Brookes.

^C Based on Bruce et al. (2013) FABM-AED application on the Yarra Estuary (Victoria); estimated from field data from Perran Cook.

^D Net flux measured during eddy correlation experiment in the Upper Swan Estuary (Kilmminster et al., 2011); varied in the range 20 – 150 mmol O₂/m²/d with a background concentration of 260 mmol O₂/m³, therefore $F_{max}^{O_2} \sim 50/(260/(260+150)) = 79$ mmol O₂/m²/d.

^E Based on benthic chamber studies showing an average net flux of 50 mmol O₂/m²/d the Upper Swan estuary (Smith et al 2007).

^F Based on Smith et al (2007) assessment of data from the Upper Swan estuary, limitation at low oxygen concentrations is not observed.

Table 14: Summary of water column biogeochemical parameter descriptions, units and typical values.

Symbol	Description	Units	Assigned value	Comment
$k_{atm}^O_2$	oxygen transfer coefficient	m/s	calculated	<i>Wanninkhof (1992)</i>
$[O_2]_{atm}$	atmospheric oxygen concentration	mmol O ₂ /m ³	calculated	<i>Riley and Skirrow (1975)</i>
$\chi_{C:O_2}^{miner, PHY}, \chi_{C:O_2}$	Stoichiometric conversion of C to O ₂	mmol C/mmol O ₂		12/32
$\chi_{N:O_2}^{nitrif}$	Stoichiometric conversion of N to O ₂	mmol N/mmol O ₂		14/32
R_{nitrif}	maximum rate of nitrification	/d	0.5	<i>Lake: 0.03 – 0.05^A; 0.037^G</i> <i>Estuary: 0.5^C</i>
K_{nitrif}	half saturation constant for oxygen dependence of nitrification rate	mmol O ₂ /m ³	78.1	<i>Lake: 62.5 – 93.7^A</i> <i>Estuary: 78.1^C</i>
θ_{nitrif}	temperature multiplier for temperature dependence of nitrification rate	-	1.08	<i>Lake: 1.08^A; 1.03^G</i> <i>Estuary: 1.08^C</i>
R_{denit}	maximum rate of denitrification	/d	0.5	<i>Lake: 0.01 – 0.04^A</i> <i>Estuary: 0.5^C</i>
K_{denit}	half saturation constant for oxygen dependence of denitrification	mmol O ₂ /m ³	21.8	<i>Lake: 12.5 – 15.6^A</i> <i>Estuary: 21.8^C</i>
θ_{denit}	temperature multiplier for temperature dependence of denitrification	-	1.08	<i>Lake: 1.05^A</i> <i>Estuary: 1.08^C</i>
R_{decom}^{PON}	maximum rate of decomposition of particulate organic nitrogen	/d	0.5	<i>Lake: 0.005 – 0.01^A; 0.03^G</i> <i>Estuary: 0.5^C</i>
K_{decom}^{PON}	half saturation constant for oxygen dependence of mineralisation rate	mmol O ₂ /m ³	31.25	<i>Lake: 47 – 78^A</i> <i>Estuary: 31.25^C</i>
θ_{decom}^{PON}	temperature multiplier for temperature dependence of mineralisation rate	-	= $\theta_{OM} = 1.08$	<i>Lake: 1.08^A</i> <i>Estuary: 1.08^C</i>
R_{miner}^{DON}	maximum rate of mineralisation of dissolved organic nitrogen	/d	0.5	<i>Lake: 0.003 – 0.05^A</i> <i>Estuary: 0.001 – 0.028^H</i>
K_{decom}^{DON}	half saturation constant for oxygen dependence of mineralisation rate	mmol O ₂ /m ³	31.25	<i>Lake: 47 – 78^A</i>
θ_{miner}^{DON}	temperature multiplier for temperature dependence of mineralisation rate	-	= $\theta_{OM} = 1.08$	1.04 – 1.10 ^A
ω_{PON}	settling rate of particulate organic matter	m/d	= $\omega_{OM} = -1.0$	<i>Estuary: -1.0^C</i>
R_{decom}^{POC}	maximum rate of decomposition of particulate organic carbon	/d	0.5	<i>Lake: 0.01 – 0.07^A; 0.008^G</i>
K_{decom}^{POC}	half saturation constant for oxygen dependence of mineralisation rate	mmol O ₂ /m ³	31.25	<i>Lake: 47 – 78^A</i>
θ_{decom}^{POC}	temperature multiplier for temperature dependence of mineralisation rate	-	= $\theta_{OM} = 1.08$	1.04 – 1.10 ^A
R_{miner}^{DOC}	maximum rate of mineralisation of dissolved organic carbon	/d	0.5	<i>Lake: 0.003 – 0.05^A</i> <i>Estuary: 0.001 – 0.006^H</i>
K_{decom}^{DOC}	half saturation constant for oxygen dependence of mineralisation rate	mmol O ₂ /m ³	31.25	<i>Lake: 47 – 78^A</i>
θ_{miner}^{DOC}	temperature multiplier for temperature dependence of mineralisation rate	-	= $\theta_{OM} = 1.08$	1.04 – 1.10 ^A
ω_{POC}	settling rate of particulate organic matter	m/day	= $\omega_{OM} = -1.0$	
R_{decom}^{POP}	maximum rate of decomposition of particulate organic phosphorus	/d	0.5	<i>Lake: 0.01 – 0.03^A; 0.099^G</i>
K_{decom}^{POP}	half saturation constant for oxygen dependence of mineralisation rate	mmol O ₂ /m ³	31.25	<i>Lake: 47 – 78^A</i>
θ_{decom}^{POP}	temperature multiplier for temperature dependence of mineralisation rate	-	= $\theta_{OM} = 1.08$	1.04 – 1.10 ^A
R_{miner}^{DOP}	maximum rate of mineralisation of dissolved organic phosphorus	/d	0.5	<i>Lake: 0.01 – 0.05^A</i>

K_{decom}^{DOP}	half saturation constant for oxygen dependence of mineralisation rate	mmol O ₂ /m ³	31.25	Lake: 47 – 78 ^A
θ_{miner}^{DOP}	temperature multiplier for temperature dependence of mineralisation rate	-	= θ_{OM} = 1.08	1.04 – 1.10 ^A
ω_{POP}	settling rate of particulate organic matter	m/d	= ω_{OM} = -1.0	
$\Phi_{ads}^{pH}(pH)$	Function characterizing pH effect on	-	calculated	-0.0088(pH) ² + 0.0347(pH) + 0.9768 ^I
c_{ads}^r	ratio of adsorption and desorption rate coefficients	l/mg		Lake: 0.7 ^J
c_{ads}^{max}	maximum adsorption capacity of SS	mmol P/mg SS		Lake: 0.00016 ^J

- ^A Converted from data on oligotrophic lakes (Romero et al. 2004) to eutrophic lakes (Gal et al. 2009), and justifications therein.
- ^C Based on Bruce et al. (2013) FABM-AED application on the Yarra Estuary (Victoria); estimated from field data from Perran Cook.
- ^G Based on Schladow & Hamilton (1997) for Prospect Reservoir.
- ^H Based on incubations by Petrone et al. (2009) for Swan Estuary (Western Australia).
- ^I Based on regression of data from Salmon et al. (submitted) based on data review from 6 papers
- ^J Based on model of Chao et al. (2010).

Table 15: Summary of phytoplankton parameter descriptions, units and example values for typical species.

parameter	description	units	Diatom	Greens	Blue-greens	Reference
R_{growth}^{PHY}	phytoplankton growth rate at 20C	/d	3.0	0.9	1.0	Various
I_K	light % saturation constant for algal limitation	$\mu\text{E m}^{-2} \text{s}^{-1}$	60	80	130	Romero et al. (2004)
I_S	saturating light intensity	$\mu\text{E m}^{-2} \text{s}^{-1}$	150	150	150	Schladow & Hamilton (1997)
θ_{growth}^{PHY}	Arrhenius temperature scaling for growth	-	1.06	1.06	1.06	Kruger and Ellof (1978), Coles and Jones (2000), Schladow & Hamilton (1997)
T_{std}	standard temperature	C	20	20	20	Griffin et al. (2001)
T_{opt}	optimum temperature	C	25	27	28	Griffin et al. (2001)
T_{max}	maximum temperature	C	32	33	35	Griffin et al. (2001)
R_{resp}^{PHY}	phytoplankton respiration rate at 20C	/d	0.085	0.085	0.085	Schladow & Hamilton (1997)
k_{fres}^{PHY}	fraction of metabolic loss that is respiration	-	0.25	0.25	0.25	Gal et al. 2009
k_{fdom}^{PHY}	fraction of metabolic loss that is DOM	-	0.2	0.2	0.2	Gal et al. 2009
θ_{resp}^{PHY}	Arrhenius temperature scaling for respiration	-	1.12	1.05	1.05	Gal et al. 2009
K_N	half-saturation concentration of nitrogen	mmol N /m ³	3.5	2.7	1.0	Gal et al. 2009
$R_{NUptake}^{PHY}$	maximum nitrogen uptake rate	mmol N /m ³ /d				
χ_{NMIN}^{PHY}	minimum internal nitrogen concentration	mmol N / mmol C				
χ_{NMAX}^{PHY}	maximum internal nitrogen concentration	mmol N / mmol C				
K_P	half-saturation concentration of phosphorus	mmol P /m ³	0.15	0.07	0.05	Gal et al. 2009
$R_{NUptake}^{PHY}$	maximum phosphorus uptake rate	mmol P /m ³ /d				
χ_{PMIN}^{PHY}	minimum internal phosphorus concentration	mmol P / mmol C				
χ_{PMAX}^{PHY}	maximum internal phosphorus concentration	mmol P / mmol C				
K_{Si}	half-saturation concentration of silica	mmol Si /m ³	2.5	-	-	Romero et al. 2004
$\chi_{C:Si}^{PHYa}$	internal silicate concentration	mmol Si / mmol C		-	-	
ω_{PHY}	phytoplankton sedimentation rate	m/d	-0.86	-0.01	-0.02	Gal et al. 2009; Romero et al. 2004
MORE...						

Table 16: Summary of zooplankton parameter descriptions, units and typical values.

parameter	description	units	Example parameter value
ε_{min}^z	Minimum zooplankton concentration	mmol C/m ³	0.1
R_{grz}^z	Zooplankton grazing rate	/day	1.5
k_{assim}^z	Assimilation efficiency for zooplankton grazing	-	0.9
K_{grz}^z	Half saturation constant for zooplankton grazing	-	40
θ_{grz}^z	Temperature multiplier for zooplankton grazing	-	1.08
T_{std}^z	Standard temperature for zooplankton grazing	°C	20.0
T_{opt}^z	Optimum temperature for zooplankton grazing	°C	22.0
T_{max}^z	Maximum temperature for zooplankton grazing	°C	30.0
p_z^z	Preference factor of zooplankton grazing on phytoplankton	-	0.7
$p_{PHY_a}^z$	Preference factor of zooplankton grazing on zooplankton	-	0.0
p_{POM}^z	Preference factor of zooplankton grazing on particulate organic matter	-	0.3
p_b^z	Preference factor of zooplankton grazing on bacteria	-	0.0
ε_{grz}^z	Concentration of prey at which grazing by zooplankton is limited	mmol C/m ³	10.0
R_{loss}^z	Respiration rate coefficient	/day	0.1
R_{mort}^z	Mortality rate coefficient	/day	0.01
k_{fecal}^z	Fecal pellet fraction of loss rate	-	0.2
k_{excr}^z	Excretion fraction of loss rate	-	0.7
k_{fsed}^z	Fraction of fecal pellets that sink directly to sediments (hard fraction)	-	0.15
θ_{loss}^z	Temperature multiplier for zooplankton loss	-	1.08
$\chi_{C:N}^z$	Ratio of internal nitrogen to carbon	mmol N / mmol C	0.2
$\chi_{C:P}^z$	Ratio of internal phosphorus to carbon	mmol P / mmol C	0.01
θ_{sal}^z	Type of salinity limitation function		1
S_{max}^z	Maximum or optimal salinity	psu	0.0
S_{min}^z	Minimum salinity	psu	35.0
S_{int}^z	Salinity intercept, for S=0	-	10.0
θ_{oxy}^z	Simulate oxygen limitation		1
ε_{oxy}^z	Minimum concentration of dissolved oxygen at which zooplankton can survive	mmol O ₂ /m ³	0.05

Configuring the AED library

All the possible state variables that can be simulated by the AED modules are listed in Table 17. Each of the variables listed below can also be specified as an output via the NetCDF output. They are generally available as a suffix to the module name, `aed_module_varname`, for example, to view oxygen search for the `aed_oxygen_oxy`. The keywords for most of the simulated variables are also used to specify the inflow boundary conditions in relevant inflow files (depending on the hydrodynamic driver).

Although there are numerous state variables in total, many are not compulsory and depend on the modules selected and how the interactions between modules are configured. This configuration is done via options outlined in the `fabm.nml` file (or `aed.nml` if FABM is not being used). An example of a AED module setup and the necessary interactions that can be configured is shown in Figure 4. For example, setting the target for excretion would be done by setting the variable:

```
n_excretion_target_variable = "aed_organic_matter_don"
```

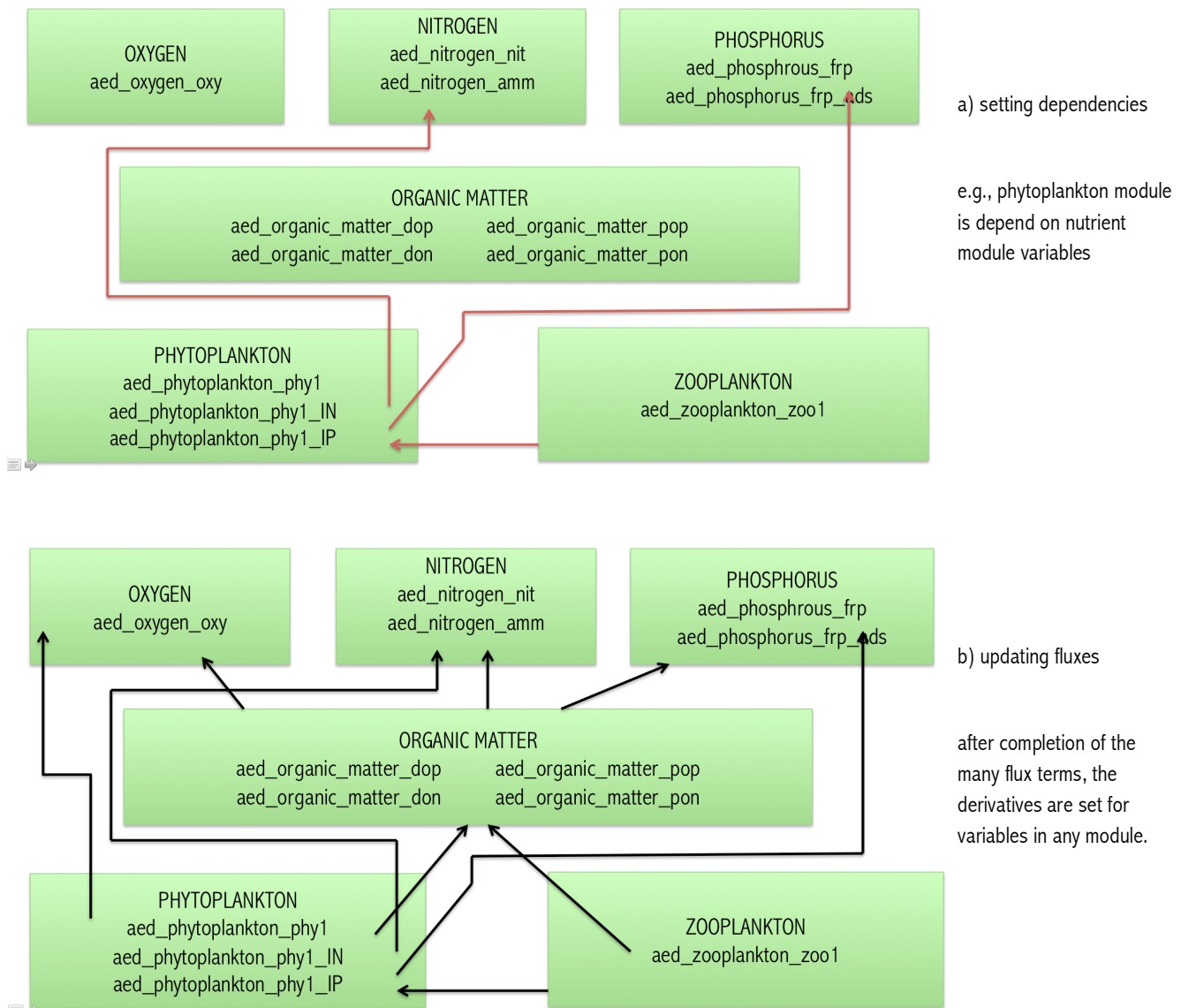


Figure 4: Example of linkages that need to be set in a AED simulation, outlining a) dependencies for a phytoplankton and zooplankton that must be configured, and b) linkages that are updated during operation of the model system.

Table 17: Current coupled aquatic biogeochemical models included within the FABM framework.

Symbol	Name	Units	AED module
General			
t	time	days	
dz	layer height	m	
A	layer/cell area	m^2	
Environmental dependencies			
T	Temperature	$^\circ\text{C}$	
S	Salinity	ppt	
I_{PAR}	Photosynthetically active radiation (PAR: 400-700nm)	W/m^2	
Oxygen			
O_2	concentration of dissolved oxygen	$\text{mmol O}/\text{m}^3$	aed_oxygen
Silica			
RSi	reactive silica (SiO_2) concentration	$\text{mmol Si}/\text{m}^3$	aed_silica
Nitrogen			
NH_4	concentration of ammonium	$\text{mmol N}/\text{m}^3$	aed_nitrogen
NO_3	concentration of nitrate	$\text{mmol N}/\text{m}^3$	aed_nitrogen
Phosphorus			
PO_4	concentration of filterable reactive phosphorus (PO_4)	$\text{mmol P}/\text{m}^3$	aed_phosphorus
PO_4^{ads}	concentration of adsorbed phosphate	$\text{mmol P}/\text{m}^3$	aed_phosphorus
Carbon			
CH_4	concentration of methane	$\text{mmol C}/\text{m}^3$	aed_carbon
DIC	concentration of dissolved inorganic carbon	$\text{mmol C}/\text{m}^3$	aed_carbon
pH	pH	-	aed_carbon
Organic Matter (DOM & POM)			
POC	concentration of particulate organic carbon	$\text{mmol C}/\text{m}^3$	aed_organic_matter
DOC	concentration of dissolved organic carbon	$\text{mmol C}/\text{m}^3$	aed_organic_matter
PON	concentration of particulate organic nitrogen	$\text{mmol N}/\text{m}^3$	aed_organic_matter
DON	concentration of dissolved organic nitrogen	$\text{mmol N}/\text{m}^3$	aed_organic_matter
POP	concentration of particulate organic phosphorus	$\text{mmol P}/\text{m}^3$	aed_organic_matter
DOP	concentration of dissolved organic phosphorus	$\text{mmol P}/\text{m}^3$	aed_organic_matter
Phytoplankton			
N_{PHY}	number of simulated phytoplankton groups	-	aed_phytoplankton
PHY_C	concentration of phytoplankton carbon	$\text{mmol C}/\text{m}^3$	aed_phytoplankton
PHY_N	concentration of phytoplankton nitrogen	$\text{mmol N}/\text{m}^3$	aed_phytoplankton
PHY_P	concentration of phytoplankton phosphorus	$\text{mmol P}/\text{m}^3$	aed_phytoplankton
PHY_{Si}	concentration of phytoplankton silica	$\text{mmol Si}/\text{m}^3$	aed_phytoplankton
Zooplankton			
N_{zoo}	number of simulated zooplankton groups	-	aed_zooplankton
ZOO	concentration of zooplankton carbon	$\text{mmol C}/\text{m}^3$	aed_zooplankton
Totals			
TN	Total nitrogen	$\text{mmol N}/\text{m}^3$	aed_totals
TP	Total phosphorus	$\text{mmol P}/\text{m}^3$	aed_totals
TSS	Total suspended solids	$\text{mg SS}/\text{m}^3$	aed_totals
$Turbidity$	Turbidity	NTU	aed_totals

In summary, currently the modules support the following process descriptions and features, and they are presented here **in order of hierarchical dependence**, which is important in setting the order of module configuration in the `fabm.nml` control file:

aed_oxygen:

- Surface/bottom exchange
- Photosynthesis / respiration
- OM mineralisation

aed_silica

- benthic flux
- phyto uptake

aed_phosphorus

- benthic flux of PO_4
- phytoplankton uptake
- organic matter mineralisation
- adsorption to inorganic particles

aed_nitrogen

- benthic flux of NO_3 and NH_4
- phytoplankton uptake
- denitrification/nitrification
- organic matter mineralisation

aed_organic_matter

- POM and DOM for C, N, and P
- Decomposition and hydrolysis of detrital material, and mineralisation
- Benthic flux of dissolved organic material
- phytoplankton production through excretion, exudation and mortality
- Multiple “pools” can be configured (eg. labile/refractory), by simulating multiple instances.

aed_chla:

- generic bulk phytoplankton module for simulating growth of chl-a

aed_phytoplankton:

- Multiple groups, support flexible setting of interactions and configuration (eg. N uptake of NH_4 , NO_3 , DON, N_2 possible)
- Uses a “parameter library file”, `aed_phyto_pars.nml`, which stores many pre-configured parameter sets that users can choose from.
- Includes numerous options for temperature, salinity, light, & nutrient environmental dependencies
- Variable IN:IP (droop) or fixed N:P (static) allowed

aed_zooplankton:

- Multiple groups can be configures to represent species/functional groups or size classes within species/functional groups.
- Physiological parameters set by user in name list: `aed_zoop_pars.nml`.
- Choice of food set in name list from phytoplankton, bacteria and particulate organic matter

aed_pathogens:

- Multiple groups can be configures to represent species/functional groups
- Processes for mortality and inactivation depending on environmental conditions, and optional growth term also included.
- Physiological parameters set by user in name list `aed_pathogen_pars.nml`.

References

- Ambrose, R.B. Jr., Wool, T.A., Conolly, J.P., and Scahnz, R.W.. 1988. A Hydrodynamic and Water Quality Model: Model Theory, Users Manual, and Programmers manual: WASP4 Environmental Research Laboratory, US EPA, EPA 600/3-87/039, Athens, GA.
- Arhonditsis, G.B., Adams-Vanharn, B.A., Nielsen, L., Stow, C.A., and Reckhow, K.H., 2006. Evaluation of the current state of mechanistic aquatic biogeochemical modeling: citation analysis and future perspectives. *Environ. Sci. Technol.*, **40**, 6547-6554.
- Bruce, L.C., Hipsey, M.R. and Cook, P.M., 2011. Quantification of sediment and water processing of nitrogen in a periodically anoxic urban estuary using a 3D hydrodynamic-biogeochemical model. *MODSIM*.
- Bruce LC, Hamilton DP, Imberger J, Gal G, Gophen M, Zohary T, Hambright KD, 2006. A numerical simulation of the role of zooplankton in C, N and P cycling in Lake Kinneret, Israel. *Ecol. Model.* **193**:412-436.
- Broekhuizen, N., Rickard, G. J., Bruggeman, J. & Meister, A. 2008. An improved and generalized second order, unconditionally positive, mass conserving integration scheme for biochemical systems. *Applied Numerical Mathematics* 58:319–40.
- Bruggeman, J. 2011. D2.14 Users guide and report for models in the MEECE library – Framework for Aquatic Biogeochemical Models (FABM). Report for the EC FP7 MEECE project 212085. 57pp.
- Burchard H et al. 2005. Application of modified Patankar schemes to stiff biogeochemical models, *Ocean Dyn*, **55**: 326-37
- Burchard, H., Bolding, K., Kuhn, W., Meister, A., Neumann, T. & Umlauf, L. 2006. Description of a flexible and extendable physical- biogeochemical model system for the water column. *Journal of Marine Systems* 61: 180-211.
- Chao, X., Jia, Y., Shields, F.D., Wang, S.S.Y., and Cooper, C.M., 2010. Three-dimensional numerical simulation of water quality and sediment-associated processes with application to a Mississippi Delta lake. *Journal of Environmental Management* **91**: 1456 – 1466.
- Chalker, B.E., 1980. Modelling light saturation curves for photosynthesis: an exponential function. *Journal of Theoretical Biology* 84, 205–215.
- Coles, J.F. and R.C. Jones. 2000. Effect of temperature on photosynthesis-light response and growth of four phytoplankton species isolated from a tidal freshwater river. *J. Phycology*, **36**: 7-16.
- Droop, M.R. 1974. The nutrient status of algal cells in continuous culture. *J. Mar. Biol. Assoc. UK*, **54**: 825–855.
- Fasham, M.J.R., Ducklow, H.W. & Mckelvie, S.M., 1990. A nitrogen-based model of plankton dynamics in the oceanic mixed layer. *J Mar Res* 48: 591-639
- Gal, G., Hipsey, M.R., Paparov, A., Makler, V. and Zohary, T., 2009. Implementation of ecological modeling as an effective management and investigation tool: Lake Kinneret as a case study. *Ecol. Model.*, **220**: 1697-1718.
- Griffin, S.L., Herzerfeld, M., Hamilton, D.P., 2001. Modelling the impact of zooplankton grazing on phytoplankton biomass during a dinoflagellate bloom in the Swan River Estuary, Western Australia. *Ecological Engineering*, **16**: 373-394.
- Hipsey, M.R., Salmon, S.U., Aldrige, K.T. and Brookes, J.D., 2010. Impact of hydro-climatological change and flow regulation on physical and biogeochemical dynamics of the Lower River Murray, Australia. *8th International Symposium on Ecohydraulics (ISE2010)*, September, 2010, Korea.
- Hipsey, M.R., and Hamilton, D.P., 2008. The Computational Aquatic Ecosystem Dynamics Model (CAEDYM): v3 Science Manual. Centre for Water Research Technical Report, Perth, Australia.
- Jassby, A.D., Platt, T., 1976. Mathematical formulation of the relationship between photosynthesis and light for phytoplankton. *Limnology and Oceanography* 21 (4), 540–547.
- Jellison, R. & Melack, J.M. 1993. Meromixis and vertical diffusivities in hypersaline Mono Lake, California. *Limnol. Oceanogr.* **38**: 1008–1019.
- Kilminster et al., 2011. Unpublished data.
- Kirk, J.T.O .1994. *Light and Photosynthesis in Aquatic Ecosystems*. Cambridge University Press.
- Klepper, O., Peters, J.C.H., Van de Kamer, J.P.G., Eilers, P., 1988. The calculation of primary production in an estuary. A model that incorporates the dynamic response of algae, vertical mixing and basin morphology. In: Marani, A. (Ed.), *Advances in Environmental Modelling*. Elsevier, pp. 373–394.
- Kromkamp, J. & Walsby, A.E. 1990. A computer model of buoyancy and vertical migration in cyanobacteria. *J. Plankton Res.* **12**: 191–183.
- Kruger, G.H.J. and J.N. Eloff. 1977. The influence of light intensity on the growth of different *Microcystis* isolates. *J. Limnol. Soc. Sth Africa*. **3**: 21-25.

- Monod (1950). Monod, J., 1950. La technique de culture continue. théorie et applications. *Annales de L Institut Pasteur* 79, 390–410.
- Mooij, W.M., Trolle, D., Jeppesen, E., Arhonditsis, G., Belolipetsky, P.V., Chitamwebwa, D.B.R., Degermendzhy, A.G., DeAngelis, D.L., De Senerpont Domis, L.N., Downing, A.S., Elliott, A.E., Fragoso Jr, C.R., Gaedke, U., Genova, S.N., Gulati, R.D., Håkanson, L., Hamilton, D.P., Hipsey, M.R., Hoen, J., Hülsmann, S., Los, F.J., Makler-Pick, V., Petzoldt, T., Prokopkin, I.G., Rinke, K., Schep, S.A., Tominaga, K., Van Dam, A.A., Van Nes, E.H., Wells, S.A., Janse, J.H., 2010. Challenges and opportunities for integrating lake ecosystem modelling approaches, *Aquatic Ecology*, **44**: 633–667.
- Petrone K.C. Richards, J.S. and Grierson, P.F., 2009. Bioavailability and composition of dissolved organic carbon and nitrogen in a near coastal catchment of south-western Australia. *Biogeochemistry*, **92**: 27–40.
- Romero, J.R., Antenucci, J.P., & Imberger, J. 2004. One- and Three- Dimensional biogeochemical Simulations of Two Differing Reservoirs. *Ecol. Model.*.
- Riley, J.P. & Skirrow, G.. 1974. Chemical Oceanography Academic Press, London.
- Robarts, R.D. and T. Zohary. 1987. Temperature effects on photosynthetic capacity, respiration and growth rates of bloom forming cyanobacteria. *N.Z. J Mar. Freshwater Res.* **21**: 391-399.
- Schladow, S.G. & Hamilton, D.P. 1997 Water quality in lakes and reservoirs. Part II Model calibration, sensitivity analysis and application. *Ecol. Model.* **96**: 111–123.
- Rhee, G.Y. & Gotham, E.J. 1981 The effect of environmental factors on phytoplankton growth: temperature and the interactions of temperature with nutrient limitation. *Limnol. Oceanogr.* **26**, pp. 635–648.
- Smith, C.S., Haese, R.R. and Evans, S. 2010. Oxygen demand and nutrient release from sediments in the upper Swan River estuary. Geoscience Australia Record, 2010/28. Commonwealth Government, Canberra.
- Smith, C.S., Murray, E.J., Hepplewhite, C. and Haese, R.R. (2007. Sediment water interactions in the Swan River estuary: Findings and management implications from benthic nutrient flux surveys, 2000-2006. Geoscience Australia Record 2007/13.
- Steele, J.H., 1962. Environmental control of photosynthesis in the sea. *Limnology and Oceanography* 7, 137–150.
- Spillman, C.M., Hamilton, D.P., Hipsey, M.R. and Imberger, J., 2008. A spatially resolved model of seasonal variations in phytoplankton and clam (*Tapes philippinarum*) biomass in Barbamarco Lagoon, Italy, *Estuarine, Coastal and Shelf Science*, **79**: 187-203.
- Spillman, C.M., Imberger, J., Hamilton, D.P., Hipsey, M.R. and Romero, J.R., 2007. Modelling the effects of Po River discharge, internal nutrient cycling and hydrodynamics on biogeochemistry of the Northern Adriatic Sea. *Journal of Marine Systems*, **68**: 127-200.
- Talling, J. F. 1957. The phytoplankton population as a compound photosynthetic system. *New Phytol.* **56**: 133-149
- Trolle, D., Hamilton, D.P., Hipsey, M.R., Bolding, K., Bruggeman, J., Mooij, W. M., Janse, J. H., Nielsen, A., Jeppesen, E., Elliott, J. E., Makler-Pick, V., Petzoldt, T., Rinke, K., Flindt, M. R., Arhonditsis, G.B., Gal, G., Bjerring, R., Tominaga, K., Hoen, J., Downing, A. S., Marques, D. M., Fragoso Jr, C. R., Søndergaard, M. and Hanson, P.C. 2012. A community-based framework for aquatic ecosystem models. *Hydrobiologia*, 683(1): 25-34.
- Wanninkhof, R.. 1992. Relationship between windspeed and gas exchange over the ocean. *J. Geophys. Res. (Oceans)* **97**(C5): 7373–7382.
- Webb, W.L., Newton, M., & Starr, D. 1974. Carbon dioxide exchange of *Alnus rubra*: a mathematical model. *Oecologia* **17**: 281–291.